Estimation of Synchronous Machine Parameters by Stand Still Frequency Responses Testing

Farid LEGUEBEDJ, and Djamel BOUKHETALA

Abstract− This paper presents a general method based on the standstill frequency response (SSFR) tests cited in IEEE Std 115-A. The used methodology consists of determining the frequency response of the measured values of the direct axis and quadrature operational inductances. Subsequently, we identify the different models of transfer functions, which are functions of time constants, using curve-fitting techniques. Then considering the time constants as inputs and the parameters of the equivalent circuits of the synchronous machine as outputs. We can identify all the parameters of different topologies of the models, using the numerical Newton Raphson method. The approach used is inexpensive, accurate, and reliable.

***Keywords*− Synchronous machine, standstill frequency responses tests, equivalent circuit, identification parameters.**

NOMENCLATURE

s	Laplace's operator
Vd	d-axis stator voltage
Vq	q-axis stator voltage
Vf	d-axis field voltage
id	d-axis stator current
if	field current
$varm$	stator voltage during test
$iarm$	stator current during test
$Zd(s)$	d-axis operational impedance
$Ld(s)$	d-axis operational inductance
Ld	q-axis synchronous inductance
Ra, Rf	stator and field resistances
Rk, Rb, Re	d-axis damper resistances
Lk, Lb, Le	d-axis magnetizing inductances
La	armature leakage inductance
Lmd	direct-axis stator to rotor mutual inductance
$Td0'$	d-axis transient open circuit time constant
Td'	d-axis transient short-circuit time constant
$Td0''$	d-axis subtransient open circuit time constant
Td''	d-axis subtransient short-circuit time (t) constant
$Td0'''$	d-axis sub-subtransient open circuit time constant
Td'''	d-axis sub-subtransient short-circuit time constant
$Td0''''$	d-axis sub-sub-subtransient open circuit t constant
Td''''	d-axis sub-sub-subtransient short-circuit t constant
G(s)	stator to field transfer function
Zafo(s)	stator to field transfer impedance

I. INTRODUCTION

Synchronous generators play a crucial role in power supply systems, and to study their stability and power control, understanding the parameters of synchronous machines is imperative [1]. Precise identification of these parameters is of utmost importance, and the literature presents various measurement techniques and identification methods for determining synchronous machine model parameters [2]. The graphical analysis of short-circuit tests [3,4] a classic method outlined in IEEE standard 115 [5] enables obtaining parameters of the d-axis but does not identify q-axis parameters. Certain investigations [6-8] based on time analysis, such as Standstill Time, Response (SSTR) and Rotating Time-Domain Response (RTDR) described in IEEE standard 115 [5], have been explored. RTDR has been employed to determine machine parameters along both axes [9,10]. The rapid evolution of computers has given rise to several identification methods for synchronous generator models. On-line measurements during normal machine operation fall into two categories: "grey box" modelling, assuming a known model structure like orthogonal series [11,25] or Kalman filter [24], and "black box" modelling, where no model structure is assumed. In the latter, the goal is solely to establish the correspondence of inputs to outputs using methods like neural networks [14, 15] or Volterra series [16]. The prevailing approach for determining d-q model parameters involves Standstill Frequency Response (SSFR) tests introduced in [17]. During SSFR tests at standstill, the machine is stationary, and the rotor aligns with the d-axis or q-axis. Two stator phases are supplied in series by a sinusoidal voltage source with variable frequency. Machine parameters are then determined through a transfer function optimization process characterizing the d-q model. In spite of the widespread use of SSFR, detailed experimental setups are seldom provided in publications [18], including technical characteristics of measuring and recording devices, frequency range and number, and the magnitude of the source voltage. Such information is vital for obtaining satisfactory measurements for data analysis. Some authors have investigated factors that can impact SSFR results, such as the level of machine magnetization during testing [19, 20] and variations in stator resistance [21]. Beyond the experimental aspects, the SSFR method encounters another challenge related to parameter identification from the collected data. Similar to any system identification problem, selecting the model type, estimator, minimization algorithm, and initial values becomes essential. The IEEE standard 1110 [22] outlines various potential structures for the d-q model, with variations primarily contingent on the number of branches employed to depict the rotor circuit in each axis based on rotor construction type [23]. In this paper, we present a general procedure, with a judicious choice of a topology of the equivalent circuit of the synchronous machine. We start by using the curve fitting techniques to obtain the suitable model, then we use the Newton Raphson method to determine the parameters of the circuit. Our paper is structured in five sections. Section II is devoted to the development of models of the synchronous machine. In section III the stand still frequency

Manuscript received April 20, 2023; revised December 20, 2023.

F. LEGUEBEDJ, D. BOUKHETALA are with Process Control Laboratory at Ecole Nationale Polytechnique, Algiers, Algeria. (e-mail: farid.leguebedj/djamel.boukhetala/@g.enp.edu.dz).

Digital Object Identifier (DOI): 10.53907/enpesj.v3i2.192

responses tests (SSFR) are presented on d-q axis for data determination. Section IV develops the general process for extracting machine parameters. In section IV we present the obtained results and their validation. Finally, the conclusion is presented in section V.

II. DIRECT-AXIS MODEL STRUCTURE OF A SYNCHRONOUS MACHINE

The determination of synchronous machine parameters from the transfer function represents the operational inductance as a function of frequency. The operational inductance is derived from the machine impedance, which is measured across the stator terminals. This method involves three main steps:

- Conversion from impedance to operational inductance.
- Determination of the time constants from the operational inductance.
- Determination of machine parameters from time constants and inductances.

The conversion from machine impedance to operational inductance is based on the direct-axis equivalent circuit of a synchronous machine, Fig. 1.

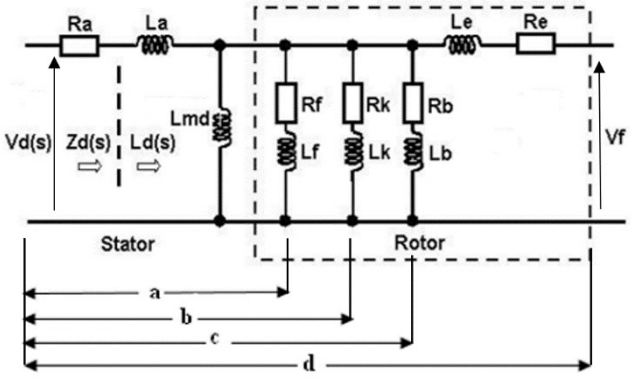

Fig. 1: Equivalent Circuit of a fourth order model for direct axis

A. Synchronous machine models

1. First order model (one rotor circuit)

The fundamental equivalent circuit is the one that incorporates one field circuit in the direct axis and one damper winding in the quadrature axis, depicted in Fig. 1.a. The operational inductance can be expressed in the following manner [12]:

$$Ld(s) = \frac{Rf(La + Lmd) + s(LaLmd + LaLf + LmdLf)}{Rf + s(Lmd + Lf)} \tag{1}$$

Equation (1) can be written in the following standard form:

$$Ld(s) = Ld\frac{(1 + sTd')}{(1 + sTd0')} \tag{2}$$

Where

$$Td' = \frac{Lf+La}{Rf} \tag{3.a}$$

$$Td0' = \frac{Lf+Lmd}{Rf} \tag{3.b}$$

$Lamd$ is the parallel combination of *Lmd* and *La,* and

$$Ld = La + Lmd \tag{3.c}$$

2. Second order model (two rotor circuits)

Figure 1.b represents the equivalent circuit of the operational inductance of the second order model. The operational inductance of this model can be written in the following form [12]:

$$Ld(s) = \frac{(La+Lmd)(Rf+sL\ )(Rk+sLk)+sLaL\quad(Rf+sLf+Rk+sLk)}{(Rf+sL\ )(Rk+sLk)+sLmd(Rf+sLf+Rk+sLk)} \tag{4}$$

By simplifying equation (4), we get:

$$Ld(s) = Ld\frac{(1 + s(Td' + T1) + s^2Td'Td'')}{(1 + s(Td0' + T2) + s^2Td0'Td0'')} \tag{5}$$

where

$$T1 = (Lk + Lamd)/Rk;$$

$$T2 = (Lk + Lmd)/Rk. \tag{6}$$

The exact time constants of the zeros and poles of equation 6 are obviously determined by extracting the roots of the quadratic equations composing the numerator and the denominator. For the denominator, the roots are:

$$S_{1,2} = \frac{-(Td0'+T2)}{2Td0'Td0''} \pm \frac{1}{2}\sqrt{\frac{Td0'+T2}{Td0'Td0''} - \frac{4}{Td0'Td0''}} \tag{7}$$

and for the numerator

$$S_{1,2} = \frac{-(Td'+T1)}{2Td'Td''} \pm \frac{1}{2}\sqrt{\frac{Td'+T1}{Td'Td''} - \frac{4}{Td'Td''}} \tag{8}$$

Therefore, the operational inductance for a second-order model can be written as:

$$Ld(s) = Ld\frac{(1 + sTd')(1 + sTd'')}{(1 + sTd0')(1 + sTd0'')} \tag{9}$$

3. Third order model (three rotor circuits)

The effect of expanding the model to include other parallel branches on the rotor for other eddy current effects, caps and slot wedges etc…. Consequently add further pole-zero pairs into the frequency response, requiring the identification of additional pairs of time constants.

When the equivalent circuit of the rotor is composed of three branches in parallel, as shown in Figure 1c, the equation of the operational inductance is naturally a ratio of polynomials of third order, for which the denominator is given by

$$\begin{aligned}\text{Den} = [1+s\left\{\frac{Lf+Lmd}{Rf} + \frac{Lk+L}{Rk} + \frac{Lb+Lmd}{Rb}\right\} + \\ s^2\left\{\frac{Lf*Lb+Lb*Lmd+Lmd*Lf}{Rf*Rb} + \frac{Lb*Lk+L\ *Lmd+Lmd*Lb}{Rb*Rk} + \right. \\ \left.\frac{Lf*Lk+L\ *Lmd+Lmd*Lk)}{Rk*Rf}\right\} + \\ \frac{s^3(Lf*Lb*Lk+L\ *Lk*Lmd+Lb*Lk*Lmd+Lb*Lf*Lmd)}{Rf*Rk*Rb}]\end{aligned} \tag{10}$$

The numerator has exactly the same shape as the denominator but with Lm replaced by Lam in each of the coefficients of s, s2 and s3.

$$\text{Num}=[1+s\left\{\frac{Lf+La}{Rf}+\frac{Lk+Lam}{Rk}+\frac{Lb+Lam}{Rb}\right\}+ s^2\left\{\frac{Lf*Lb+Lb*Lam+Lam*Lf}{Rf*Rb}+\frac{Lb*Lk+Lk*Lam+Lam*Lb}{Rb*Rk}+\frac{Lf*Lk+Lf*Lam+Lam*Lk)}{Rk*Rf}\right\}+ \frac{s^3(Lf*Lb*Lk+\quad *Lk*Lam+Lb*Lk*Lam+Lb*Lf*Lam)}{Rf*Rk*Rb}](La+ Lmd) \quad (11)$$

And

$$Ld(s)=\frac{Num}{Den} \quad (12)$$

So the operational inductance for a third-order model can be expressed as:

$$Ld(s)=Ld\frac{(1+sTd')(1+sTd'')(1+sTd''')}{(1+sTd0')(1+sTd0'')(1+sTd0''')} \quad (13)$$

4. Fourth order model (fourth rotor circuits)

The equivalent circuit of the fourth-order model is shown in Figure 1.d. It follows from the previous analyzes that the transfer function of each model is constructed by adding a pair of zero poles to the lower model. The operational inductance is given by:

$$Ld(s)=Ld\frac{(1+sTd')(1+sTd'')(1+sTd''')(1+sTd'''')}{(1+sTd0')(1+sTd0'')(1+sTd0''')(1+sTd0'''')} \quad (14)$$

III. STANDSTILL FREQUENCY RESPONSE TESTS

Standstill frequency response testing is highly recommended for obtaining synchronous machines parameters compared to short-circuit testing methods. There are three mains reasons that show the superiority of this method they are

- The capability to determine the parameters of the both axes, the direct axis and the quadrature axis.
- The ability to identify the parameters of higher order models.
- The results obtained using sudden short circuit tests are only relevant for the second order model (two rotor circuits). In addition these tests remain unable to determine the synchronous machines parameters in the q-axis.

The following subsections describe the general procedure of the SSFR method, as given in reference [5].

1. *Measurable quantities*

The d and q axis operational impedances are respectively

$$Zd(s)=Ra+sLd(s) \quad (15)$$

$$Zq(s)=Ra+sLq(s) \quad (16)$$

To obtain the frequency response characteristics of the operational quantities, the following measurements are made:

$$Zd(s)=\frac{\Delta Vd(s)}{s\Delta id(s)}\Big|\ \Delta Vf=0 \quad (17)$$

$$Zq(s)=\frac{\Delta Vq(s)}{s\Delta iq(s)}\Big|\ \Delta Vf=0 \quad (18)$$

$$G(s)=\frac{\Delta Vd(s)}{s\Delta Vf(s)}\Big|\ \Delta Vf=0 \quad (19)$$

From the equations (16) and (17) above, the operational inductances in d-q axis can be written as follows

$$Ld(s)=\frac{Zd(s)-Ra}{s} \quad (20)$$

$$Lq(s)=\frac{Zq(s)-Ra}{s} \quad (21)$$

The stator resistance Ra is defined by

$$Ra=\lim_{s\to 0}|Zd\,(s)| \quad (22)$$

Or by

$$Ra=\lim_{s\to 0}|Zq\,(s)| \quad (23)$$

We can also measure $sG(s)$. The principle of this test is based on measuring small variations in field and armature current when the field circuit is shorted as shown in equation (24).

$$sG(s)=\frac{\Delta if(s)}{s\Delta id(s)}\Big|\Delta Vf=0 \quad (24)$$

In addition, the armature to the field transfer impedance $Zafo$ is measured, as follows

$$Zafo(s)=-\frac{\Delta Vf(s)}{s\Delta if(s)}\Big|\ \Delta if=0 \quad (25)$$

2. *Measurement setup*

The typical configuration of SSFR tests is composed of a sinusoidal signal generator, a power amplifier, the MUT (machine under test) and an analyzer capable of measuring at the same time the amplitude and phase differences of two input signals. The four schemes below show the test configurations of the measurable quantities $Zd(s)$, $Zq(s)$, $sG(s)$ and $Zafo(s)$. We note that the frequency range varies from 0.001 Hz to 1000 Hz.

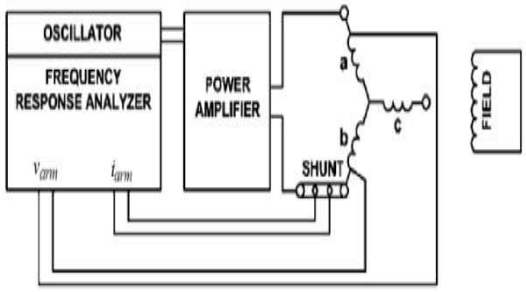

Fig. 2: Test schematic for the d-axis operational impedance, $Zd(s)$

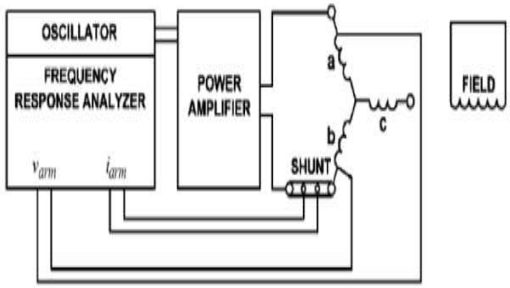

Fig. 3: Test schematic for the q-axis operational impedance, $Zq(s)$

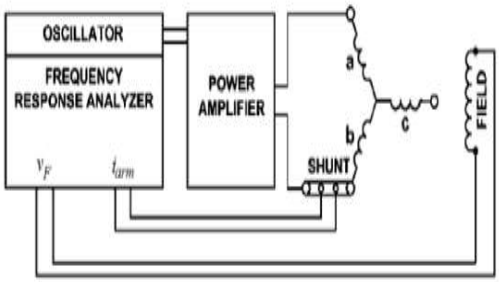

Fig. 4: Test schematic for the stator to field transfer function, $sG(s)$

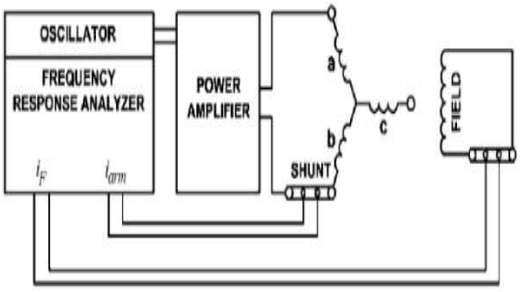

Fig. 5: Test schematic for the stator to field transfer impedance, $Zafo(s)$

IV. METHODOLOGY

The design methodology proposed in this study begins with the definition of the structure of the d-axis equivalent circuits. We are interested in the SSFR1, SSFR2, and SSFR3 models, it should be noted that this methodology can be correctly applied to any circuit topology for the q axis.

1. D-axis parameters from tests

In order to implement our method, a machine with a power of 277.8 MVA and a voltage of 16.5 KV was chosen. SSFR results are published in EPRI [13] and d-axis impedance has been introduced for the process of identifying the parameters of synchronous machine models. Fig. 6 represents the experimental measurements of the impedance *Zd(s)*.

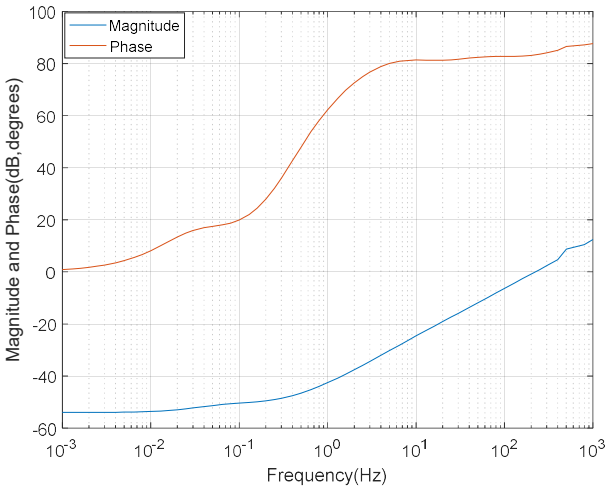

Fig. 6: Frequency response of the impedance (measured data)

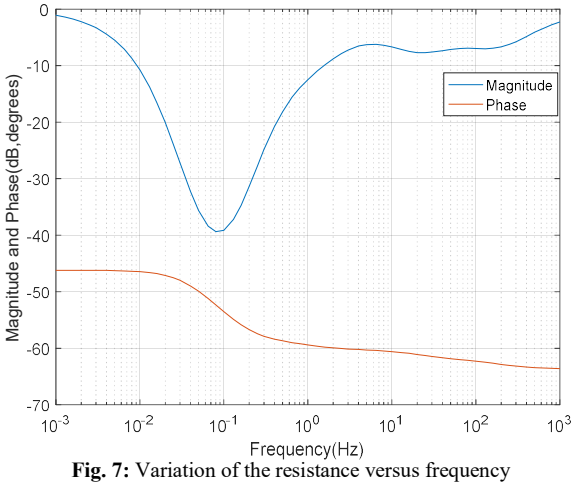

Fig. 7: Variation of the resistance versus frequency

By extrapolating the real part of the operational impedance at zero frequency, we obtain the stator resistance value $Ra = 0.002000\ \Omega$, Fig. 7. Equation (21) makes it possible to trace the evolution of operational inductance magnitude in dB and its phase in degree. The extrapolation of the operational inductance $Ld(s)$ at zero frequency, allows calculating the synchronous inductance value $Ld = -46{,}1991$ dB $= 0.004898$ H, Fig. 8.

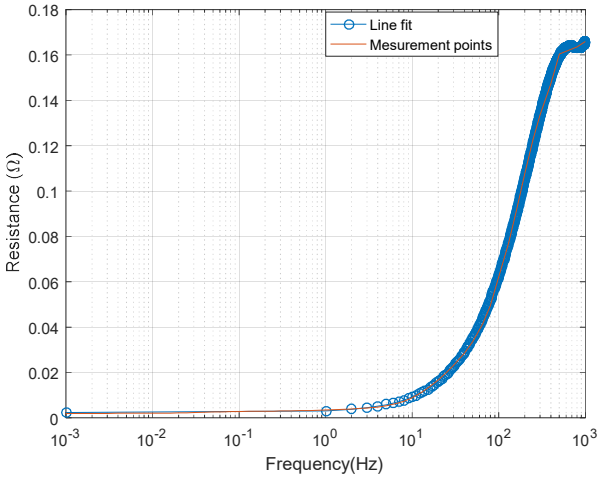

Fig. 8: Frequency response of the operational inductance in terms of magnitude (in dB) and phase in (degrees)

The mutual inductance of the stator in the direct axis to the rotor can be obtained by taking the difference between the d-axis synchronous inductance and the leakage inductance as follows:

$$Lmd = Ld - La \quad (26)$$

The choice of the value of the leakage inductance in the technical literature [14] is taken $La = 8\%\ Ld$.

2. D-axis equations set

In this part, we try to find the relations between the time constants of the operational inductance and the parameters of the equivalent circuit of synchronous machine models. In this context, we are interested in the third order model (SSFR3). We proceed to the development of equation (13), then by identifying it with equations (10) and (11), we obtain the non-linear equations system, whose inputs are the time constants and outputs are the parameters of the equivalent circuit.

The system is:

$$Lam = \frac{La*Lmd}{La+Lmd} \quad (27)$$

$$Td' + Td'' + Td''' = \frac{Lf+Lmd}{Rf} + \frac{Lk+Lmd}{Rk} + \frac{Lb+Lmd}{Rb} \quad (28)$$

$$Td' * Td'' + Td'' * Td''' + Td''' * Td' = \frac{Lk * Lf + Lb * Lmd + Lf * Lmd}{Rf * Rb} + \frac{Lb * Lk + Lj * Lmd + Lk * Lmd}{Rb * Rk} + \frac{Lf * Lk + Lf * Lmd + Lk * Lmd}{Rk * Rf} \quad (29)$$

$$Td' * Td'' * Td''' = \frac{Lf*Lb*Lk+Lb*Lk*Lmd+Lf*Lk*Lmd+Lf*Lb*Lmd}{Rf*Rb*Rk} \quad (30)$$

$$Td0' + Td0'' + Td0''' = \frac{Lf+Lam}{Rf} + \frac{Lk+Lam}{Rk} + \frac{Lb+Lam}{Rb} \quad (31)$$

$$Td0' * Td0'' + Td0'' * Td0''' + Td0''' * Td0' = \frac{Lk * Lf + Lb * Lam + Lf * Lam}{Rf * Rb} + \frac{Lb * Lk + Lb * Lam + Lk * Lam}{Rb * Rk} + \frac{Lf * Lk + Lf * Lam + Lk * Lam}{Rk * Rf} \quad (32)$$

$$Td0' * Td0'' * Td0''' = \frac{Lf*Lb*Lk+Lb*Lk*Lam+L\ *Lk*Lam+Lf*Lb*Lam}{Rf*Rb*Rk} \quad (33)$$

3. Identifying direct Axis model time constants

Curve fitting techniques are used here, to identify the time constants of the models from the measured data of operational inductance magnitude and phase. The 'freqs' and 'invfreqs' functions in MATLAB convert measured data from the frequency response of the operational inductance to a transfer function for different models.

The following results were obtained with MATLAB:

First order model (SSFR1)

$$Ld(s) = 0.004500\frac{(1 + 0.491032s)}{(1 + 2.301883)} \quad (35)$$

Second order model (SSFR2)

$$Ld(s) = 0.004898\frac{(1 + 0.820584s)(1 + 0.005902s)}{(1 + 3.858375s)(1 + 0.008495s)} \quad (36)$$

Third order model (SSFR3)

$$Ld(s) = 0.004899\frac{(1 + 0.896976s)(1 + 0.084855s)(1 + 0.002473s)}{(1 + 3.944719s)(1 + 0.101208s)(1 + 0.003354s)} \quad (37)$$

4. Determination of equivalent circuit parameters

The set of nonlinear equations outlined in subsection III.2 underwent simulation through the Newton Raphson method in MATLAB, utilizing the time constants from the previously identified third-order model (SSFR3). This methodology was also employed to deduce the parameters of the SSRF1 and SSFR2 models.

While this method is simple and easy to execute, a significant drawback is its susceptibility to converging towards a local minimum based on the chosen model and initial values. The progression of SSFR3 model parameters over iterations, illustrates that total convergence is achieved around the 8th iteration, Fig. 9 to Fig. 14.

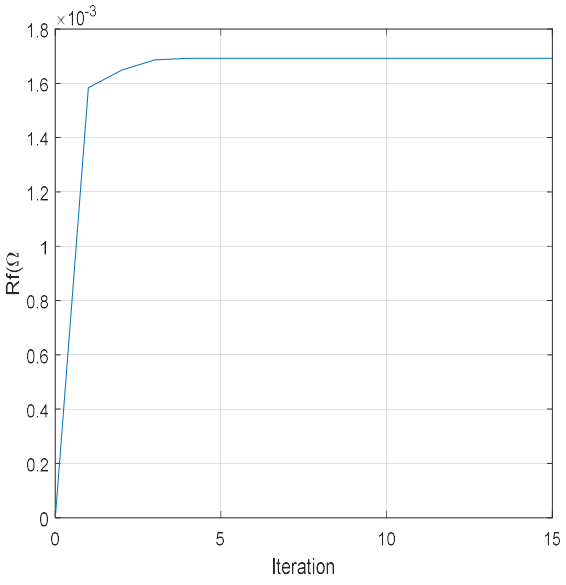

Fig. 9: Variation of resistance Rf versus Iteration

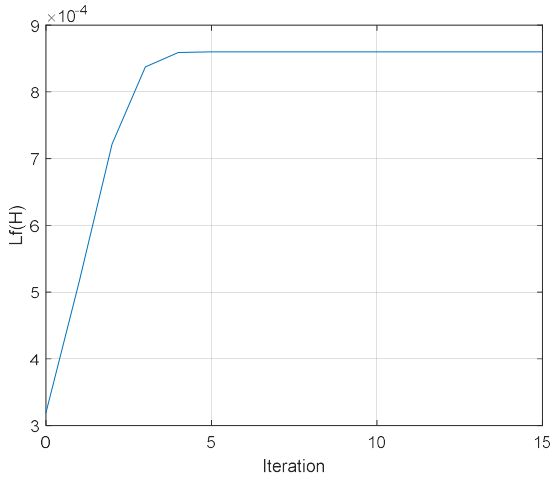

Fig. 10: Variation of inductance Lf versus Iteration

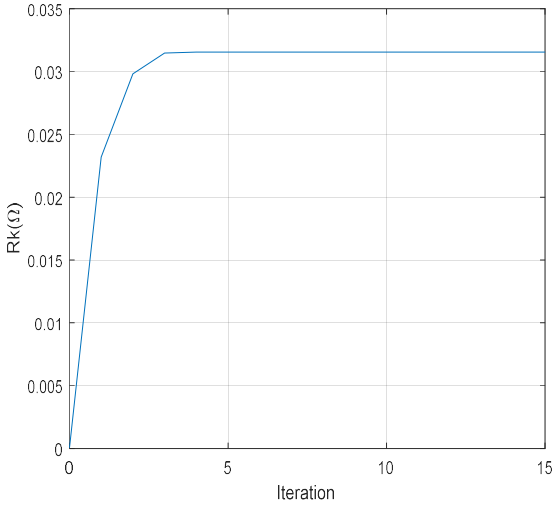

Fig. 11: Variation of resistance Rk versus Iteration

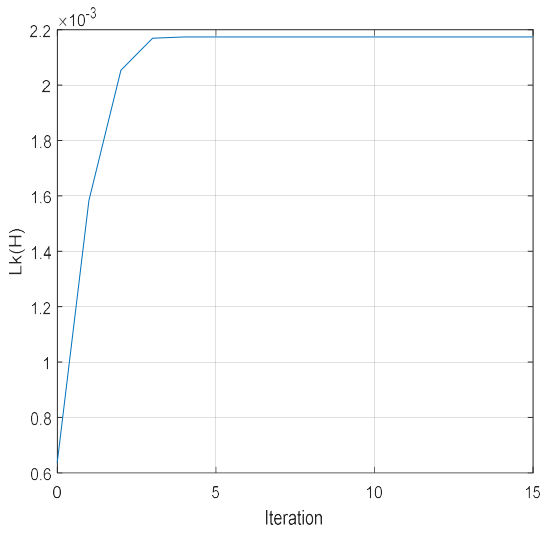

Fig. 12: Variation of inductance Lk versus Iteration

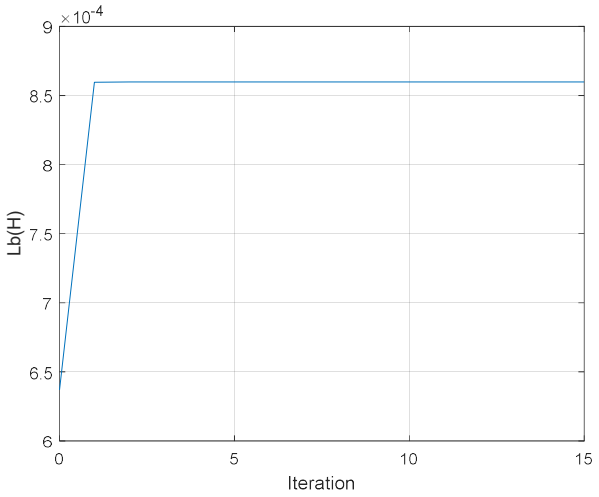

Fig. 13: Variation of resistance Rb versus Iteration

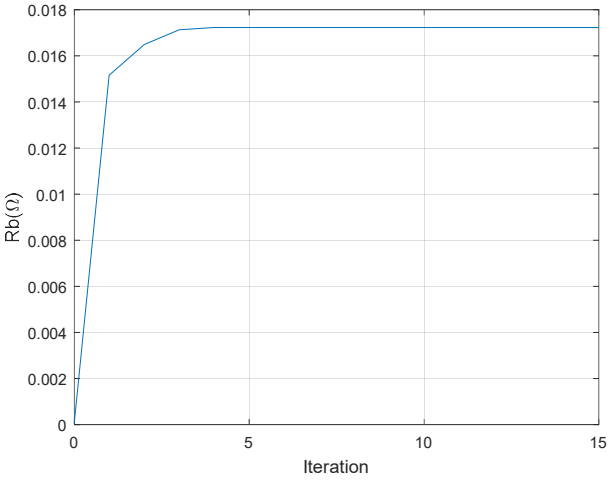

Fig. 14: Variation of inductance Lb versus Iteration

The parameters of the equivalent circuits of models SSFR1, SSFR2, and SSFR3 are summarized in Table 1:

Table 1. Estimation of equivalent circuits parameters

parametrs	SSFR1 model	SSFR2 model	SSFR3 model
Rf (Ω)	0.0026169	0.0011697	0.001692
Lf (H)	0.000842	0.000759	0.000859
Rk (Ω)	-	0.194508	0.017233
Lk (H)	-	0.000672	0.000859
Rj (Ω)	-	-	0.031553
Lj (H)	-	-	0.002174

V. RESULTS AND VALIDATION

In order to validate the results obtained, the parameters estimated using the Newton Raphson method for SSFR1, SSFR2, and SSFR3 models, as outlined in Table 1, are incorporated into the transfer functions represented by equations (1), (4), and (12) respectively. The resulting findings

are illustrated in Figures 15 and 16. A direct comparison between the frequency responses of these models and the measured data distinctly showcases the effectiveness of the proposed approach. Upon closer examination of the curves in Figures 15 and 16, it becomes apparent that the SSFR2 model outperforms the other models. A notable resemblance is evident between the frequency response of this particular model and the measured data.

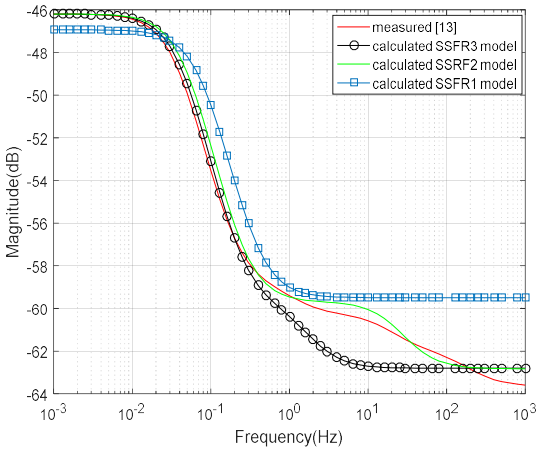

Fig. 15: Operational inductance magnitude versus frequency

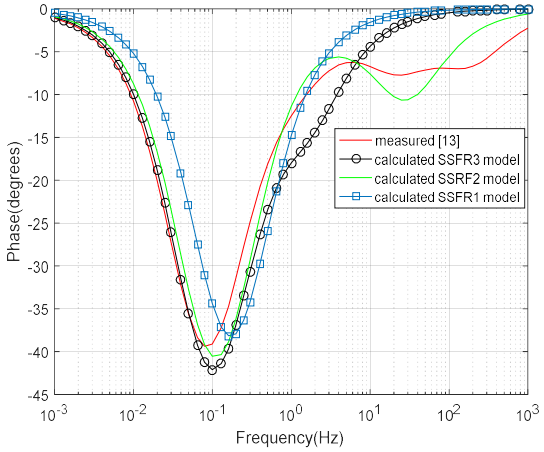

Fig. 16: Operational inductance phase versus frequency

5. CONCLUSION

This study introduced a methodology for computing parameters in the direct axis equivalent circuits of synchronous machines, demonstrating its applicability to various models. The values derived from this approach align well with experimentally reported data. In evaluating the frequency response, the phase discrepancy between the SSFR2 model and measured data for operational inductance ranges from -3.78 degrees to 2.75 degrees, with a magnitude error fluctuating between -0.34 dB and 0.77 dB. It was observed that implementing this method is straightforward, rapid, comprehensible, and reproducible.

REFERENCES

[1] Aghamohammadi, M. R., A. Beik Khormizi, and M. Rezaee, "Effect of generator parameters inaccuracy on transient stability performance," Power and Energy Engineering Conference (APPEEC), 1-5, Mar. 2010.

[2] Ghomi, M. and Y. N. Sarem, "Review of synchronous generator parameters estimation and model identification," 2007 42nd International Universities Power Engineering Conference, 228-235, 2007.

[3] Kamwa, I., M. Pilote, H. Carle, P. Viarouge, B. Mpanda-Mabwe, and M. Crappe, "Computer software to automate the graphical analysis of sudden – short - circuit oscillograms of large synchronous machines," IEEE Trans. Energy Convers., Vol. 10, No. 3, 399-406, Sep. 1995.

[4] Kamwa, I., P. Viarouge, and R. Mahfoudi, "Phenomenological models of large synchronous machines from short-circuit tests during commissioning-a classical/modern approach," IEEE Trans. Energy Convers., Vol. 9, No. 1, 85-97, Mar. 1994.

[5] "IEEE guide for test procedures for synchronous machines part iacceptance and performance testing Part II. Test procedures and parameter determination for dynamic analysis," IEEE Std 115-2009 Revis. IEEE Std 115-1995, 1-219, May 2010.

[6] Sellschopp, F. S. and M. A. Arjona, "DC decay test for estimating d-axis synchronous machine parameters: A two-transfer-function approach," IEE Proc. – Electr. Power Appl., Vol. 153, No. 1, 123-128, Jan. 2006.

[7] Sellschopp, F. S. and M. A. Arjona, "Semi-analytical method for determining d-axis synchronous generator parameters using the dc step voltage test," IEE Proc.– Electr. Power Appl., Vol. 1, No. 3, 348-354, May 2007.

[8] Maurer, F., T. Xuan, and J. Simond, "Tow full parameter identification methods for synchronous machine applying DC-decays tests for a rotor in arbitrary position," IEEE Transactions on Industry Applications, Vol. 53, No. 4, 3505-3518, Jul.-Aug. 2017.

[9] Wamkeue, R., C. Jolette, and I. Kamwa, "Advanced modeling of a synchronous generator under line-switching and load-rejection tests for isolated grid applications," IEEE Trans. Energy Convers., Vol. 25, No. 3, 680-689, Sep. 2010.

[10] Hiramatsu, D., M. Kakiuchi, K. Nagakura, Y. Uemura, K. Koyanagi, K. Hirayama, S. Nagano, R. Nagura, and K. Nagasaka, "Analytical study on generator load rejection characteristic using advanced equivalent circuit," 2006 IEEE Power Engineering Society General Meeting, 18-22, Montreal, QC, Jun. 2006.

[11] Melgoza, J. J. R., G. T. Heydt, A. Keyhani, B. L. Agrawal, and D. Selin, "An algebraic approach for identifying operating point dependent parameters of synchronous machines using orthogonal series expansions," IEEE Trans. Energy Convers., Vol. 16, No. 1, 92-98, Mar. 2001.

[12] F. Leguebedj, D. Boukhetala, and M. Tadjine, "An Optimization Analytical Method for Synchronous Machine Model Design from Operational Inductance Ld(s)," Progress In Electromagnetics Research B, Vol. 97, pp. 115-130, 2022.

[13] Electric Power Research Institute, "Compendium of the EPRI Workshop on determination of synchronous machine stability study constants," by N. E. I Parsons, Aug. 1980.

[14] Shariati, O., A. A. M. Zin, and M. R. Aghamohammadi, "Application of neural network observer for on-line estimation of salient-pole synchronous generator's dynamic parameters using the operating data," 2011 4th International Conference on Modeling, Simulation and Applied Optimization (ICMSAO), 1-9, 2011.

[15] Henrique, L., D. Kornrumpf, and S. I. Nabeta, "Determination of synchronous parameters through the SSFR test and artificial neural networks," The 9th International Conference on Power Electronics, Machines and Drives (PMD 2018), 2018.

[16] Fard, R. D., M. Karrari, and O. P. Malik, "Synchronous generator model identification using Volterra series," IEEE Power Engineering Society General Meeting, Vol. 2, 1344-1349, 2004.

[17] Sen, S. K. and B. Adkins, "The application of the frequency response method to electrical machines," Proc. IEE, Vol. 103, No. 4, 378-391, 1956.

[18] Belqorchi,A.,U.Karragac, J. Mehseredjian, and I. Kamwa, "Standstill frequency response test and validation of a large Hy-drogenerator," IEEE Transactions on Power Systems, Vol. 34, No. 3, 2261-2269, May 2019, ISSN: 0885-8950, DOI: 10.1109/TPWRS.2018.2889510.

[19] Sellschopp, F. S. and M. A. Arjona, "Determination of synchronous machine parameters using standstill frequency response tests at different excitation levels," 2007 IEEE International Electric Machines & Drives Conference, Vol. 2, 1014-1019, 2007.

[20] Kutt, F., S. Racewicz, and M. Michna, "SSFR test of synchronous machine for different saturation levels using finite-element method," IECON 2014– 40th Annual Conference of the IEEE Industrial Electronics Society, 907-911, 2014.

[21] Radjeai, H., A. Barakat, S. Tnani, and G. Champenois, "Identification of synchronous machine by Standstill Frequency Response (SSFR) method influence of the stator resistance," 2010 XIX International Conference onElectrical Machines (ICEM), 1-5, 2010. 22.

[22] "IEEE guide for synchronous generator modeling practices and applications in power system stability analyses," IEEE Std 1110-2002 Revis. IEEE Std 1110-1991, 1-72, 2003.

[23] Dandeno, P. L. and A. T. Poray, "Development of detailed turbogenerator equivalent circuits from standstill frequency response measurements," IEEE Trans. Power Appar. Syst., Vol. 100, No. 4, 1646-1655, Apr. 1981.
[24] Rengifo, C. F., C. Gir_on, J. Palechor, A. Diego, and M. Bravo, "Identification of a synchronous generator parameters using recursive least squares and Kalman filter," 20 Revista
[25] Melgoza, J. J. R., G. T. Heydt, A. Keyhani, B. L. Agrawal, and D. Selin, "Synchronous machine parameter estimation using the Hartley series," IEEE Trans. Energy Convers., Vol. 16, No. 1, 49-54, Mar. 2001.

Farid LEGUEBEDJ graduated in electrical engineering in 1989 and received the Magister degree in electrical engineering from the Ecole Nationale Polytechnique, Algiers, Algeria, in 1993. He is an Assistant Professor at Ecole Nationale Polytechnique since 1994.

Djamel BOUKHETALA graduated in automation in 1989 and received the Magister and Ph.D. degrees in automatic control from the Ecole Nationale Polytechnique, Algiers, Algeria, in 1993 and 2002, respectively. From 1996 to 1999, he was the Head of the Department of Automatic Control. He was the Director of the Control Process Laboratory from 2005 to 2013 and the Director of Postgraduate Studies and Scientific Research at ENP from 2010 to 2019. He is currently a Full Professor in automatic control with ENP. He is currently a member of several scientific councils in higher education and scientific research institutions. His research interests are decentralized control, nonlinear control, fuzzy control, and artificial neural network control applied to robotics, smart grids, and industrial process.